Eur Phys J A (2004) **19**, s01, 189–196
Digital Object Identifier (DOI) 10.1140/epjad/s2004-03-032-x

EPJ A direct
electronic only

Quark matter in neutron stars

Marcello Baldo

INFN, and Dipartimento di Fisica dell' Universita' di Catania, via S. Sofia 64, 95123 Catania, Italy

Received: 7 Aug 2003 / Accepted: 14 Nov 2003 /
Published Online: 6 Feb 2004 –

Abstract. The density of nuclear matter in the interior of neutron stars can reach values, for the largest masses, which can be compatible with the onset of hadron deconfinement. For the study of this possibility the only viable method at present is the comparison between the available nucleon and quark Equations of State (EoS) at increasing baryon density. It is then possible to trace the transition to the deconfined phase or the appearence of a mixed phase. We present recent results on the structure of neutron stars based on this procedure. For the nucleon matter, the microscopic many-body theory of the Nuclear Equation of State is discussed in the framework of the Bethe-Brueckner-Goldstone method. The expansion is extended up to the three hole-line diagrams contribution. For the quark matter, different models are used to generate the quark EoS. Despite the maximum mass of neutron stars turns out to be only marginally sensitive to the considered quark EoS, it is found that the structure of neutron stars can drastically depend on the adopted model.

PACS. 21.65+f Nuclear matter – 97.60,JD Neutron Stars – 26.60+c Nuclear aspects of Neutron Stars – 24.10,Cn Many-body

1 Introduction

From a hystorical point of view, the nuclear saturation problem was the main motivation for the extensive studies, which have lasted for few decades, on infinite nuclear matter, since it is one of the fundamental problems in nuclear physics. However, infinite nuclear matter cannot be considered only an idealized system, since it is commonly believed that macroscopic portions of (asymmetric) nuclear matter form the interior bulk part of neutron stars (NS), usually associated with pulsars. The internal structure of NS is therefore directly linked to the Equation of State (EoS) of infinite nuclear matter. An accurate prediction of the EOS is highly demanded for most studies of neutron stars and related astrophysical applications. Of course, only indirect observations of NS structure are possible. However, the astrophysics of neutron stars is rapidly developing, in view of the observations coming from the new generation of artificial satellites, and one can expect that it will be possible in the near future to confront the theoretical predictions with more and more stringent phenomenological data.

At the hadronic level, several many-body theories and techniques have been developed and applied to the study of the nuclear Equation of State. The main difficulty in the many-body theory of nuclear matter is the treatment of the strong repulsive core, which dominates the short range behaviour of the nucleon-nucleon (NN) interaction. Simple perturbation theory cannot of course be applied, since the matrix elements of the interaction are too large. One way of overcoming this difficulty is to introduce the two-body scattering G-matrix, which has a much smoother behaviour even for large repulsive core. It is possible to rearrange the perturbation expansion in terms of the reaction G-matrix, in place of the original bare NN interaction, and this procedure is systematically exploited in the Bethe-Brueckner-Goldstone (BBG) expansion [1].

For quark matter, no calculation is available at the high baryon density which is encountered in neutron star interior. For the same reason, no theory, based on QCD, is available to describe the possible transition form hadron matter to the deconfined quark matter. At present, the only viable method to explore the possible appearence of the deconfined phase in tne core of neutron stars is the use of a well defined model for the quark-gluon plasma and the comparison of the corresponding EoS with the hadronic one to assess the possible phase transition (including eventually a mixed phase). In Sect. 2 we describe the hadronic EoS and its properties at increasing density. In Sect. 3 we confront this EoS with the quark EoS obtained within few models, and we extract the NS structure for each adopted quark matter model. It turns out that, while the maximum NS mass is only slightly dependent on the quark matter model, the NS structure is strongly dependent on it.

2 The BBG expansion and the nuclear EOS

The BBG expansion for the ground state energy at a given density, i.e. the EOS at zero temperature, can be ordered according to the number of independent hole-lines appear-

ing in the diagrams representing the different terms of the expansion. This grouping of diagrams generates the so-called hole-line expansion [2]. The diagrams with a given number n of hole-lines are expected to describe the main contribution to the n-particle correlations in the system. At the two hole-line level of approximation the corresponding summation of diagrams produces the Brueckner-Hartree-Fock (BHF) approximation, which incorporates the two particle correlations. The BHF approximation includes the self-consistent procedure of determining the single particle auxiliary potential, which is an essential ingredient of the method. Once the auxiliary self-consistent potential is introduced, the expansion is implemented by introducing the set of diagrams which include "potential insertions". To be specific, the introduction of the auxiliary potential can be formally performed by splitting the hamiltonian in a modified way from the usual one

$$H = T + V = T + U + (V - U) \equiv H_0' + V' \qquad (1)$$

where T is the kinetic energy and V the nucleon-nucleon interaction. Then one consider $V' = V - U$ as the new interaction potential and H_0' as the new single particle hamiltonian. Then, the single particle energy $e(k)$ is given by

$$e(k) = \frac{\hbar^2 k^2}{2m} + U(k) \qquad (2)$$

while U must be chosen in such a way that the new interaction V' is, in some sense, "reduced" with respect to the original one V, so that the expansion in V' should be faster converging. The introduction of the auxiliary potential turns out to be essential, otherwise the hole-expansion would be badly diverging. The total energy E can then be written as

$$E = \sum_k e(k) + B \qquad (3)$$

where B is the interaction energy due to V'. The BHF sums the so called "ladder diagrams". The summation of these diagrams can be performed by solving the integral equation for the Brueckner G-matrix

$$\langle k|_1 k_2|G(\omega)|k_3 k_4\rangle\!\rangle = \langle k|_1 k_2|v|k_3 k_4|\,\rangle + \\ + \sum_{k_3' k_4'} \langle k|_1 k_2|v|k_3' k_4'\rangle\!\rangle \frac{\big(1-\Theta_F(k_3')\big)\big(1-\Theta_F(k_4')\big)}{\omega - e_{k_3'} - e_{k_4'}} \cdot \\ \langle k|_3' k_4'|G(\omega)|k_3 k_4|\,\rangle \qquad (4)$$

where $\Theta_F(k) = 1$ for $k < k_F$ and is zero otherwise, being k_F the Fermi momentum. The product $Q(k,k') = (1-\Theta_F(k))(1-\Theta_F(k'))$, appearing in the kernel of (4), enforces the scattered momenta to lie outside the Fermi sphere, and it is commonly referred as the "Pauli operator". This G-matrix can be viewed as the in-medium scattering matrix between two nucleons. The self-consistent single particle potential $U(k)$ is determined by the equation

$$U(k) = \sum_{k'<k_F} \langle k|k'|G(e_{k_1} + e_{k_2})|kk'|_\rangle A \qquad (5)$$

with $|kk'|_\rangle A = |kk'|-\rangle|kk'|\rangle$.

The first potential insertion diagram cancels out the potential part of the single particle energy of (2), in the expression for the total energy E. This is actually true for any definition of the auxiliary potential U. At the two hole-line level of approximation, one therefore gets

$$E = \sum_{k<k_F} \frac{\hbar^2 k^2}{2m} + \frac{1}{2}\sum_{k,k'<k_F} \langle k|k'|G(e_k + e_{k'})|kk'|_\rangle A \\ \equiv \sum_{k<k_F} \frac{\hbar^2 k^2}{2m} + \frac{1}{2}\sum_{k<k_F} U(k) \qquad (6)$$

The result that only the unperturbed kinetic energy appears in the expression for E, and all the correlations are included in the potential energy part, holds true to all orders and it is a peculiarity of the BBG expansion. Of course, the modification of the momentum distribution, and therefore of the kinetic energy, is included in the interaction energy part, but it is treated on the same footing as the other correlation effects. This seems to present a noticeable advantage. In fact, the modification of the kinetic energy in itself is quite large and, of course, positive and should be therefore compensated by an extremely accurate calculations of the (negative) correlation energy. On the other hand, putting the two effects on the same footing, one can expect that strong cancellation occur order by order.

The BHF results indicate that already the two hole-line approximation is able to produce reasonable values for the saturation point. The remaining discrepancies can be summarized in the celebrated Coester band [3], the line along which the results for different "realistic" nucleon-nucleon forces appear to be approximately concentrated and which misses the phenomenological saturation point. According to the force used, either the saturation density is too high or the binding energy is too small. However, the results depend on the very definition of the single particle potential. The "standard" choice for $U(k)$ assumes that the potential is zero above the Fermi momentum k_F, while in the "continuous choice" [4] the definition of (5) is extended to momenta k larger than k_F, thus making U a continuous function through the Fermi surface. The final result of a hypothetically exact BBG calculation is independent of the auxiliary potential $U(k)$, but the rate of convergence can of course depend on the particular choice adopted. Therefore, the degree of dependence of the results on the choice of the potential can be considered an indication of the degree of convergence obtained at a given level of the BBG expansion. The results for both choices of $U(k)$ at the BHF level of approximation (Argonne v_{18} potential [5]) is reported in Fig. 1 in the case of symmetric nuclear matter (solid lines). As one can see, the saturation curves are different for the two prescriptions. It has to be noticed, however, that the apparent discrepancy of 4-5 MeV in the binding energies shown in Fig. 1, is about 10% of the calculated potential energy per particle, which is about -40 MeV around saturation. This is the degree of convergence obtained at the Brueckner level. In view of these results, obtained within the BHF approximations, it appears mandatory to consider the three hole-line diagrams. The value of their contribution can indeed

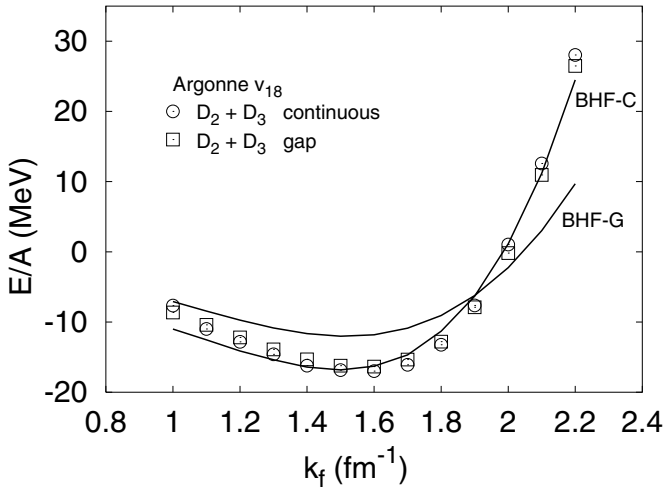

Fig. 1. Nuclear matter saturation curve for the Argonne v_{18} NN potential. The *solid lines* indicate the results at the Brueckner (*two hole-lines*) level for the standard (BHF-G) and the continuous choices (BHF-C) respectively. The results obtained adding the *three hole-line* contribution are given by the *open squares* (*standard choice*) and the *open circles* (*continuous choice*)

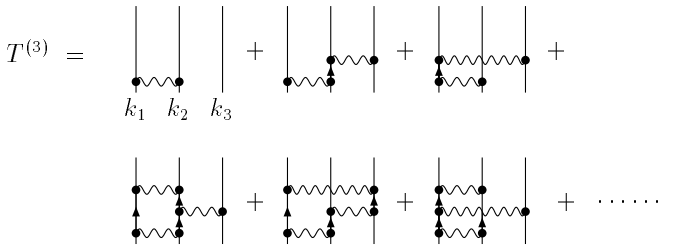

Fig. 2. The first few terms in the expansion of the Bethe-Fadeev integral equation

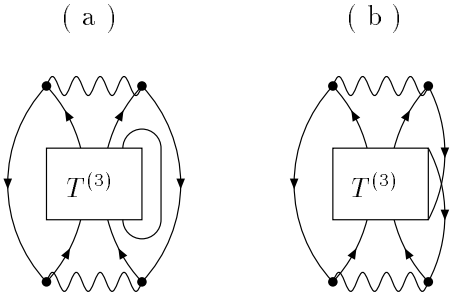

Fig. 3. Schematic representation of the direct **a** and exchange **b** three hole-line diagrams

provide a check of convergence and possibly an accurate EOS. According to the BBG expansion, this set of diagrams describes the irreducible three-nucleon correlations, i.e. the three-body correlations which cannot be reduced to a product of two-body correlations, already introduced at the BHF level. Since the two hole-line contribution has been summed up by introducing the G-matrix, the in-medium two-body scattering matrix, it is conceivable that the three hole-line diagrams can be summed up by introducing some similar generalization of the scattering matrix for three particles. The three-body scattering problem has a long history by itself, and has been given a formal solution by Fadeev [6]. For identical particles the original three integral Fadeev equations reduce to one, because of symmetry. The analogous equation and scattering matrix in the case of nuclear matter (or other many-body systems in general) has been introduced by Bethe [7]. The integral equation, the Bethe–Fadeev equation, reads schematically

$$\langle k|_1 k_2 k_3|T^{(3)}|k'_1 k'_2 k'_3|\,\rangle = \langle k|_1 k_2|G|k'_1 k'_2|\delta\rangle_K (k_3 - k'_3) + \\ + \langle k|_1 k_2 k_3|G_{12}\, X\, \tfrac{Q_3}{e}\, T^{(3)}|k'_1 k'_2 k'_3|\,\rangle \quad . \tag{7}$$

As one can see, the kernel contains the two-body scattering matrix G in place of the bare NN interaction, in line with the BBG scheme. The factor Q_3/e is the analogous of the similar factor appearing in the integral equation for the two-body scattering matrix G, see (4). Therefore, the projection operator Q_3 imposes that all the three particle states lie above the Fermi energy, and the denominator e is the appropriate energy denominator, namely the energy of the three-particle intermediate state minus the entry energy ω, in close analogy with the equation for the two-body scattering matrix G of (4). The real novelty with respect to the two-body case is the operator X. This operator interchanges particle 3 with particle 1 and with particle 2, $X = P_{123} + P_{132}$, where P indicates the operation of cyclic permutation of its indices. It gives rise to the so-called "endemic factor" in the Fadeev equations, since it is an unavoidable complication intrinsic to the three-body problem in general. The reason for the appearance of the operator X in this context is that no two successive G matrices can be present in the same pair of particle lines, since the G matrix already sums up all the two-body ladder processes. In other words, the G matrices must alternate from one pair of particle lines to another, in all possible ways, as it is indeed apparent from the expansion by iteration of (7), which is represented in Fig. 2. Adding all terms with an arbitrary number of G-matrices, one gets a generalized ladder series for three-particles, analogous to the ladder series introduced for the two particles case in defining the G-matrix. Indeed, this is the basis for the integral (7). The introduction of the three-body scattering matrix $T^{(3)}$ allows to sum up the three hole-line diagrams, as schematically indicated in Fig. 3. Here the diagrams have been divided into two distinct groups, the directs ones (a) and the exchange ones (b).

Once the first interaction has occurred, the remaining part of the diagram describes the rescattering, in all possible way, of three particle-lines, since no further hole-line must be present in the diagram. This part of the diagram is indeed the three-body scattering matrix $T^{(3)}$, and the operator Q_3 in (7) assures, as already mentioned, that only particle lines are included. The set of diagrams indicated in part (b) can be obtained by the ones of part (a) by simply interchanging the final (or initial) point of one of the "undisturbed" hole-line with the final (or initial) point of the third hole-line. This means that one can obtain each

graph of the group depicted in Fig. 3b by acting with the operator X on the bottom of the corresponding graph of Fig. 3a. Once the Bethe-Fadeev equations are solved, the contribution of the direct three hole-line diagrams of Fig. 3a can be written as

$$E_{3h}^{dir} = \tfrac{1}{2} \sum_{k_1,k_2,k_3 \le k_F} \sum_{\{k'\},\{k''\} \ge k_F} \langle k|_1 k_2|G|k'_1 k'_2|\rangle A \cdot$$

$$\cdot \tfrac{1}{e} \ \langle k|'_1 k'_2 k'_3|XT^{(3)}X|k''_1 k''_2 k''_3|\,\rangle \ \tfrac{1}{e'} \ \langle k|''_1 k''_2|G|k_1 k_2|\rangle A \quad , \tag{8}$$

In (8) the denominator $e = e_{k'_1} + e_{k'_2} - e_{k_1} - e_{k_2}$, and analogously $e' = e_{k''_1} + e_{k''_2} - e_{k_1} - e_{k_2}$. The exchange diagrams of Fig. 3b can be obtained by multiplying the same expression by a further factor X. In summary, the entire set of three hole-line diagrams can be obtained by multiplying the expression of (8) by $1+X$. A scheme of approximation was first devised by B.D. Day [8] within the gap choice for the single particle potential. In this scheme the first diagram in each one of the series (a) and (b) in Fig. 3, the so-called "bubble" and "ring" diagrams, are singled out from the whole set of three hole-line diagrams, while the remaining series of diagrams is summed up by solving the Bethe-Fadeev integral equation. This procedure turns out to be numerically convenient. We have checked [9] and extended these calculations to the continuous choice for the single particle potential. In the latter case a potential insertion diagram has to be added at the three hole-line level of approximation [1,9]. The final equation of State obtained by adding the three hole-line contribution is reported in Fig. 1, both for the gap choice (squares) and the continuous choice (stars) [10], again for the Argonne v_{18} potential. Two conclusions can be drawn from these results. i) The two saturation curves in the gap and continuous choices, with the inclusion of the three hole-line diagrams, tend now to collapse in a single EOS, with some deviations only at the highest density. This is a strong indication that a high degree of convergence has been reached at this level of the expansion, according to the criterion discussed above. Notice that the saturation curves extend from a density which is about one half of saturation density to about five times saturation density, and, therefore, it appears unlikely that the agreement between the two choices can be considered as a fortuitous coincidence. ii) The Brueckner two hole-line EOS within the continuous choice turns out to be already close to the full EOS, since in this case the three hole-line contribution is quite small. In first approximation one can adopt the BHF results with the continuous choice as the nuclear matter EOS. Indeed, this is a further indication of convergence. The phenomenological saturation point for symmetric nuclear matter is, however, not reproduced, which confirms the finding in [8]. The binding energy per particle at the minimum of the saturation curve turns out to be close to the empirical value of about -16 MeV, but the corresponding density comes out about 20-30 % larger than the empirical one. The discrepancy can be accounted for by introducing three-body forces and relativistic effects. The latter, if treated within the Dirac-Brueckner scheme, can be cosidered as a special case of three-body forces [11]. The possibility of extracting thrre-body forces, consistently with the two-body forces, has been considered both within the meson-nucleon theory of nuclear forces [12,13] and within the chiral perturbation theory [14]. A simpler method is to adopt a phenomenological form of three-body forces [15], and this is the scheme used in the calculations presented in the next Section.

3 Neutron stars and the onset of quark matter

The nuclear matter equation of state is the fundamental input for building models of neutron stars. These compact objects, among the densest in the universe, are indeed characterized by values of the baryon density which ranges from the iron density at the surface up to eight-ten times normal nuclear matter density in the core. Therefore a detailed knowledge of the equation of state over a wide range of densities is required [16]. As we have seen in the previous section, the EOS of nucleon matter can be established up to densities relevant to neutron star studies. At increasing densities an additional complication arises. In fact, whereas at densities close to the saturation value the matter consists mainly of nucleons and leptons, at higher densities several species of particles may appear due to the fast rise of the nucleon chemical potentials. The Brueckner-Hartree-Fock scheme must be then generalized to include a possible fractions of hyperons, like Λ and Σ^-. An additional uncertainity comes from our limited knowledge of the nucleon-hyperon (NY) interaction, which we describe within the Nijmegen soft-core model [17]. No hyperon-hyperon interaction was taken into account, since no robust experimental data are available yet. For more details, the reader is referred to [18,19] and references therein. In Fig. 4 we show the chemical composition of β-stable and asymmetric nuclear matter containing hyperons (panel (a)) and the corresponding equation of state (panel (b)). The shown calculations have been performed using the Paris potential. We observe that hyperon formation starts at densities $\rho \simeq 2-3$ times normal nuclear matter density. The Σ^- baryon appears earlier than the Λ, in spite of its larger mass, because of the negative charge. The appearance of strange particles has two main consequences, i) an almost equal percentage of nucleons and hyperons are present at highest densities and ii) a strong deleptonization of matter, since it is energetically convenient to maintain charge neutrality through hyperon formation than β-decay. The equation of state is displayed in panel (b). The dotted line represents the case when only nucleons and leptons are present in stellar matter, whereas the solid line shows the case when hyperons are included as well. In the latter case the equation of state gets very soft, since the kinetic energy of the already present baryonic species is converted into masses of the new particles, thus lowering the total pressure.

The relation of NS mass with the matter EoS is apparent in the Tolman-Oppenheimer-Volkoff (TOV) [16],

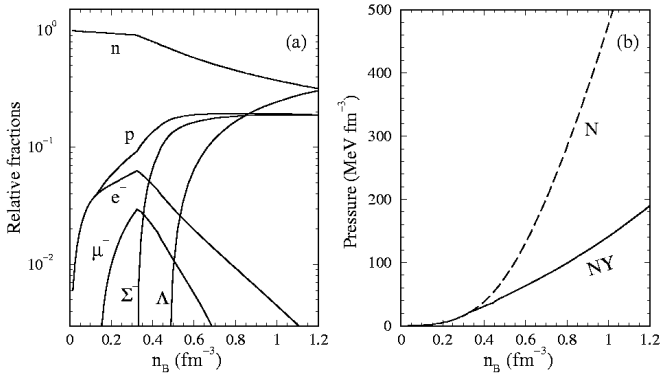

Fig. 4. In panel **a** we display the equilibrium composition of asymmetric and β-stable nuclear matter containing Σ^- and Λ hyperons. In panel **b** the *solid (dotted) line* represents the EoS obtained in the case when nucleons plus hyperons (*only nucleons*) are present

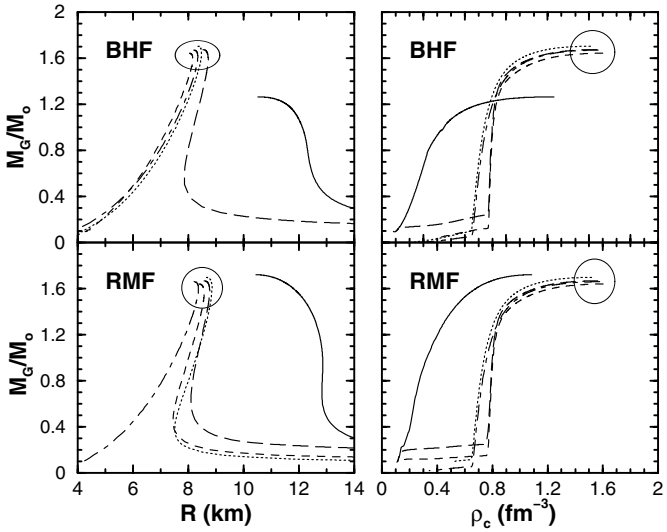

Fig. 5. The mass-radius (*left panel*) and the mass-central density (*right panel*) relations for $\epsilon_B = 0.8$ GeV fm^{-3}, see the text, and various parametrizations of the bag constant as a function of density. The *solid lines* indicate the resukts for the pure hadronic EoS discussed in the text

which determines the hydrostatic equilibrium configuration of the star (assumed to be spherically symmetric). The mass distribution is obtained by solving the TOV equations for the pressure $P(r)$ and for the mass $m(r)$ enclosed inside the sphere of radius r,

$$\frac{dP(r)}{dr} = -\frac{Gm(r)\epsilon(r)}{r^2}\,\frac{[1+P(r)/\epsilon(r)]\left[1+4\pi r^3 P(r)/m(r)\right]}{1-2Gm(r)/r}$$
$$\frac{dm(r)}{dr} = 4\pi r^2 \epsilon(r) \tag{9}$$

being G the gravitational constant and ϵ the energy density. The EoS establishes a relation between pressure and energy density, making this set of two coupled equations closed. Therfore, starting with a central mass density $\epsilon(r=0) \equiv \epsilon_c$, one integrates out until the pressure on the surface equals the one corresponding to the density of iron. This gives the stellar radius R and the corresponding gravitational mass M. It has to be noticed that the NS mass which is observable is the gravitational mass, given by

$$M_G \;\equiv\; m(R) = 4\pi \int_0^R dr\; r^2 \epsilon(r) \tag{10}$$

For the description of the NS crust, if present, one usually joins the hadronic equations of state with the ones by Negele and Vautherin [20] in the medium-density regime, and the ones by Feynman-Metropolis-Teller [21] and Baym-Pethick-Sutherland [22] for the outer crust.

However, the formation of a large fraction of strange matter at high density, and therefore in the interior of NS, can be only a hypothetical scenario, since another process can compete : the onset of a deconfined quark matter phase at large enough baryon density. This possibility has been considered recently by several authors, within specific models for the quark phase, and we will review briefly their findings.

The simplest quark matter model, widely used in model calculations, is the MIT bag model [23]. The model contains mainly two parameters, the bag constant B and the strange quark mass m_s, besides the strong coupling constant α_S which describes possible perturbative corrections. A systematic study of NS structure, as the parameters are varied, has been presented in [24]. In this work, no strange matter is considered in the hadronic sector, whose EoS is described either within the relativistic mean field or within the non-relativistic many-body model of [25]. In the quark sector, the possibility of color superconductivity (CS) [26,27] is also considered (for a review on CS see [28].) Despite the presence of strong color superconductivity (gap $\Delta \sim 100$ MeV) can enhance appreciably the NS maximum mass, one of the main conclusions of this systematic study is that the NS mass cannot exceed values of about 1.6–1.7 solar mass. A larger value of the mass would require values of the bag constant so small to make symmetric nuclear matter unstable towards deconfinement even at saturation density. This results appears in agreement with our previous work [29, 30], where also the MIT bag model was used (without color superconductivity), in conjunction with the above discussed hadron EoS, which includes strangeness. Without the quark phase, our EoS would produce a maximum mass below the observational limit of 1.44 solar mass [31]. Mixed phase, along the general method of [32], was also included. The bag constant was allowed to vary with density, in order to tune the value of the baryon energy density ϵ_B at which deconfinement occurs in symmetric nuclear matter. If this value is restricted in a "reasonable interval" , i.e. $0.8 < \epsilon_B < 1.5$ GeV fm^{-3}, the resulting maximum mass depends only weakly on ϵ_B, and it does not exceed 1.7 solar mass. These findings are summarized in Figs. 5, 6, and 7

It has to be noticed that for the largest masses, as in [24] the NS is mainly composed of pure quark matter (hybrid star). This can be seen in Fig. 8, where QP indicates

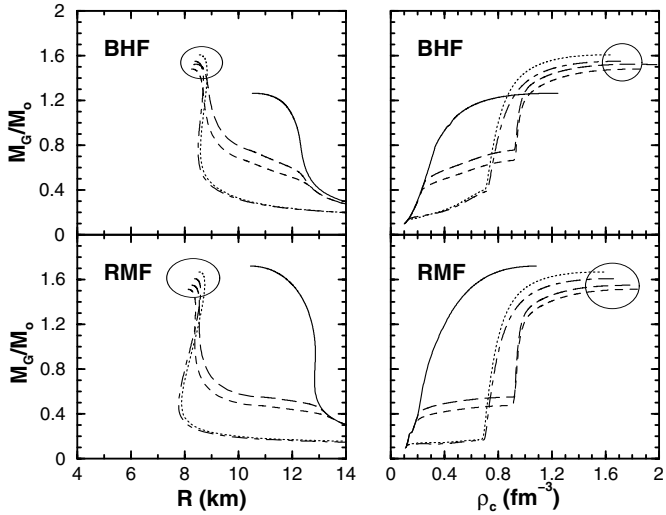

Fig. 6. The same as in Fig. 5, but for $\epsilon_B = 1.1$ GeV fm^{-3}, see the text

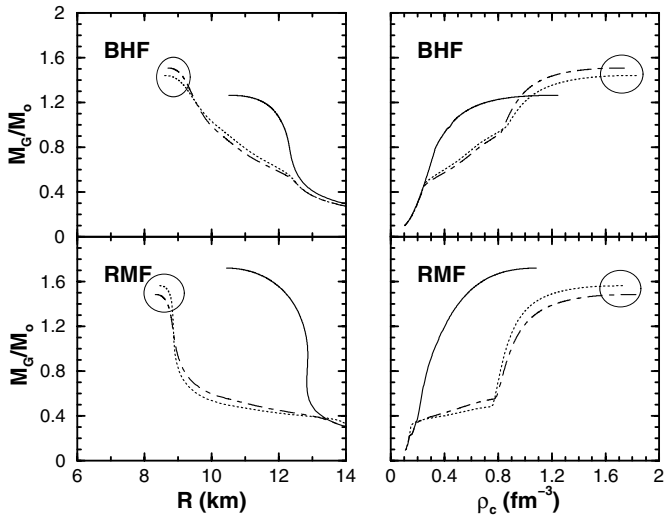

Fig. 7. The same as in Fig. 5, but for $\epsilon_B = 1.5$ GeV fm^{-3}, see the text

pure quark phase, MP the mixed phase and HP the pure hadronic phase. Comparison is also made with a similar calculation where a relativistic mean field (RMF) EoS is used for the hadronic phase (including hyperons) [33,34]. According to [24], a strong color superconductivity can even render a pure quark mass possible.

A more microscopic model for the deconfined quark phase, which has some direct links with hadron phenomenology, is the Nambu-Jona Lasinio (NJL) model [35]. The parameters of the model are held fixed to the ones fitted to reproduce the masses of the meson octet. The NJL model generates dynamically the quark masses as a function of baryon density, through the presence of the quark condensate. The model has been generalized to include also color superconductivity [36]. The latter is also dynamically generated (gap equations), and therefore it does not introduce further parameters, since the value of the pairing gap is a well defined function of the baryon density.

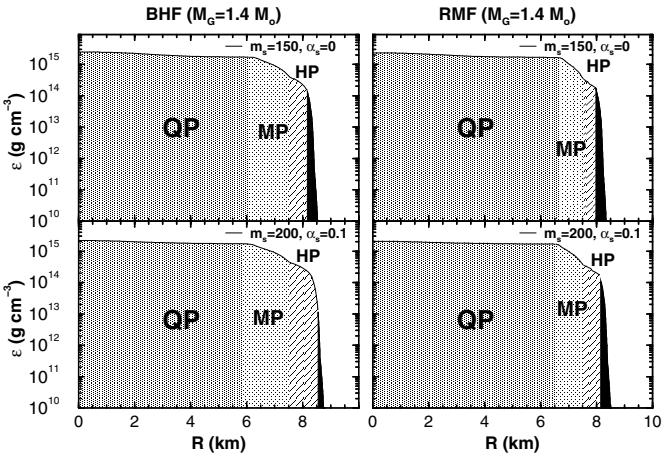

Fig. 8. Density profile of the different phase inside neutron stars when the MIT bag model is used for the quark phase. See the text for details

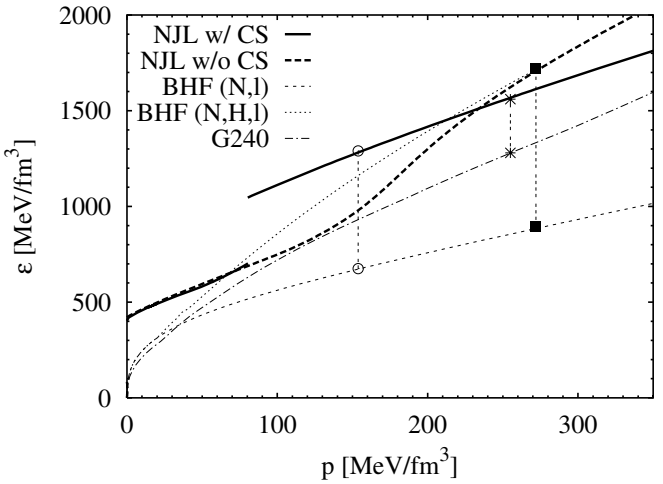

Fig. 9. Hadronic and quark matter equation of State. *Dashed line* indicates the hadron EoS without hyperons, the *dotted one* with hyperons. The *dashed-dotted line* indicates the EoS of the relativistic mean field with compressibility $K = 240$ MeV, see the text. Finally, the Eos for the NJL quark model with and without color superconductivity are indicated by the *bold solid and bold dashed lines* respectively. The points mark the values of the pressure where the corresponding hadron-quark phase transitions occur

Th resulting EoS for beta-stable neutron star matter is reported in Fig. 9, where for the hadron sector the EoS discussed above, see Fig. 4, is adopted.

The quark color superconductivity can actually appear in two different phase, the so-called two-flavour (2SC) phase, where only up and down quark partecipate, and the color-flavor locked (CFL) phase, where also the strange quark is included in a coherent combination with the other two quarks. The transition from the 2SC to the CFL phase occurs at a density (or pressure) where only the confined hadronic phase is present. The transition is responsible of the (almost) discontinuity of the quark EoS around $p \approx 100$ MeV/fm^3 in Fig. 9. Without color superconductivity, bold dashed line in Fig. 9, the EoS has, of course,

a completely smooth behaviour. The different behaviour with and without CS of the quark EoS is due not only to the additional pairing energy but also to the different density dependence of the dynamically generated quark masses and the relative quark fractions, particularly for the strange quark. The phase transition from hadron to quark matter, that was assumed to be sharp for simplicity, is marked by the points and the corresponding vertical lines which join the different EoS. The transition from hadronic to superconducting quark matter occurs around $p \approx 160$ MeV/fm^3 (open circles), while, if the CS is excluded, the transition occur (full squares) at much higher pressure (and density).

If strange matter is allowed also in the hadonic phase, according to the EoS of Fig. 4, then no transition to quark matter is possible before the NS maximum mass is reached. As we have seen, the value of the maximum mass is in this case too low, which means that this particular EoS is not acceptable. This result does not exclude the possible appearence of hadronic matter with a strange component (hyperons), since the adopted EoS is strongly dependent on the particular hyperon-nucleon interaction used in the microscopic calculations. The interaction is not so well known, especially at density above saturation. Indeed, if one adopts the EoS of [37] (version with $K = 240$ MeV), derived within the relativistic mean field approximation, which also contains hyperon components, the transition to quark matter (with CS) is now possible, since this EoS is stiffer. The corresponding value of the transition pressure is marked by the stars in Fig. 9. This EoS differ from the previous one only in the region of density where hyperons are present, while it is quite similar in the pure nucleon sector. This is because the nucleon-hyperon effective interaction is less attractive, and therefore the hyperon content is smaller and the EoS is stiffer.

Once the EoS for NS matter is obtained, the NS density and composition profile can be obtained. The results for the total mass as a function of radius are summarized in Fig. 10. As already mentioned, the EoS of Fig. 4 which includes hyperons (dotted line) produces a too law maximum mass, with no possible transition to quark matter. If hyperon are not included, within the same scheme, and quark matter is described in the NJL model with no CS (bold dashed line), the maximum mass is substantially enhanced (about 1.8 solar mass). It has to be noticed that as soon as quark matter appears at increasing central density (or decreasing radius) just at the center, the NS becomes unstable toward collapse. Since we are considering a sharp transition between the two phases (no mixed phase), the transition produces the small kink at the maximum of the mass vs. radius curve which is apparent in Fig. 10. The inclusion of a mixed phase would smooth out this behaviour and only slightly modify the value of the maximum mass [38]. This result means also that the use of the NJL model for the quark phase actually does not allow any NS with a pure quark matter core. Possibly, only a small portion of mixed phase at the center would be possible.

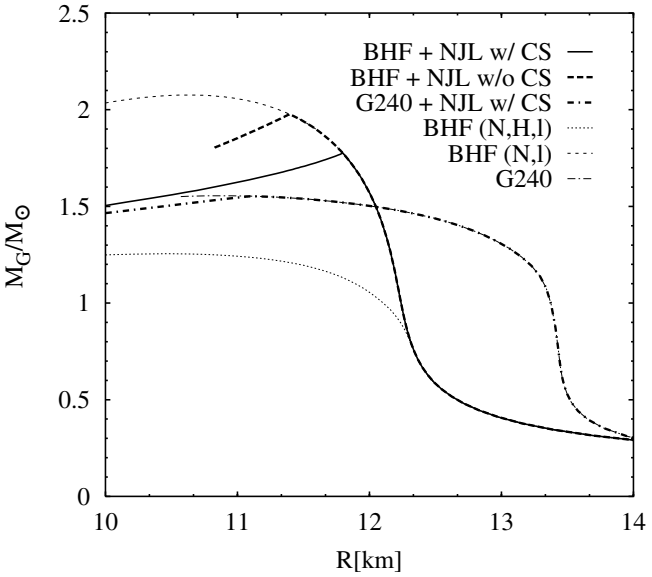

Fig. 10. Gravitational masses of comapct stars as a function of the radius for the different EOS shown in Fig. 9

This conclusion holds true also when CS is introduced in the quark phase (bold line). The effect of the CS is to reduce appreciably the maximum mass, which is in this case around 1.75 solar mass. Again, the presence of a mixed phase is expected to reduce slightly this value.

If the EoS of [37] is used, where also hyperons are included, keeping the same EoS for the quark (i.e. NJL with CS), the maximum mass further decreases to a value close to 1.55 solar mass, while the radius reduces substantially (by about 10%), making the object more compact. It can be then expected that a generic hadronic EoS with strangeness would produce a maximum mass lower than the value without strangeness, i.e. below about 1,75 solar mass. Indeed, an EoS with larger strangness content is expected to be softer, as we have seen in the discussion above.

4 Conclusions

We have discussed the results of NS structure calculations based, on one hand on a hadronic EoS which has been derived from microscopic many-body calculations, and on the other on simplified models for the possible quark phase in the core of the NS. The quark matter models include the MIT bag model and the Nambu-Jona Lasinio model, both with and without the possibility of color superconductivity. In all the calculations analysed, the maximum mass of NS never exceed values of 1.7 - 1.8 solar mass. Fot hybrid stars, i.e. stars which contain both hadronic and quark components, color superconductivity tends to reduce slightly the maximum mass. If CS is strong enough, even pure quark stars are possible for the MIT bag model. However, the structure of NS in the MIT and NJL models is drastically different. While the major fraction of NS is composed by quark matter for the MIT model, in the case of the NJL model just the onset of quark matter in

the core is able to make the NS unstable toward collapse. This means that in the latter case no pure quark matter phase could, in principle, exist in NS. This sharp difference of structure should have some effects on different properties of NS, like cooling, glitches, magnetic and rotational properties, neutrino physics, and so on. The possibility of getting a clean signal from observational data on the possible presence of quark matter in NS is still one of the main filed of research in NS physics, but, unfortunately, is also one of the most controversial. More theoretical investigations and observational data will hopefully clarify in the future this fundamental issue in the physics of NS and in the physics of high density baryonic matter.

It has to be noticed, anyhow, that in all model explored so far the NS maximum mass never exceed 1.7-1.8 solar mass. Therefore, the observation of a NS with a mass substantially larger than this value would put serious constraints on the EoS of quark matter at high density.

Acknowledgements. The material presented in this contribution is the result of a fruitful collaboration, lasting for several years, with a number of people. Special thanks are due to Dr. I. Bombaci, Dr. G.F. Burgio, Prof. L.S. Ferreira, Dr. G. Giansiracusa, Prof. U. Lombardo, Dr. P.K. Sahu, Dr. H.-J. Schulze and Prof. H.Q. Song.

References

1. For a pedagogical introduction: see *Nuclear Methods and the Nuclear equation of State*, Edited by M. Baldo, World Scientific, Singapore, International Review of Nuclear Physics Vol. 9, 1999
2. B.D. Day: *Brueckner–Bethe Calculations of Nuclear Matter*, Proceedings of the School E. Fermi, Varenna 1981, Course LXXIX, ed. A. Molinari, (Editrice Compositori, Bologna, 1983), p. 1–72; Rev. Mod. Phys. **39**, 719 (1967)
3. F. Coester, S. Cohen, B.D. Day, and C.M. Vincent: Phys. Rev. C **1**, 769 (1970); B.D. Day: Comments Nucl. Part. Phys. **11**, 115 (1983)
4. J.P. Jeukenne, A. Lejeunne, and C. Mahaux: Phys. Rep. C **25**, 83 (1976); M. Baldo, I. Bombaci, L.S. Ferreira, G. Giansiracusa, and U. Lombardo: Phys. Rev. C **43**, 2605 (1991)
5. R.B. Wiringa, V.G.J. Stocks, and R. Schiavilla: Phys. Rev. C **51**, 38 (1995)
6. L.D. Fadeev: *Mathematical Aspects of the Three-Body Problem in Quantum Scattering Theory*, Davey, New York 1965
7. R. Rajaraman and H. Bethe: Rev. Mod. Phys. **39**, 745 (1967)
8. B.D. Day: Phys. Rev. C **24**, 1203 (1981); Phys. Rev. Lett. **47**, 226 (1981)
9. H.Q. Song, M. Baldo, G. Giansiracusa, and U. Lombardo: Phys. Rev. Lett. **81**, 1584 (1998)
10. M. Baldo, A. Fiasconaro, G. Giansiracusa, and U. Lombardo e H. Q. Song: Phys. Rev. C **65**, 017303 (2001)
11. G.E. Brown, W. Weise, G. Baym, and J. Speth: Comm. Nucl. Part. Phys. **17**, 39 (1987)
12. J. Fuyita and H. Miyazawa: Progr. in Theor. Phys. **17**, 360 (1957); C. Hadjuk, P.U. Sauer, and W. Streuve: Nucl. Phys. A **405**, 581 (1983)
13. P. Grangé, A. Lejeune, M. Martzolff, and J.-F. Mathiot: Phys. Rev C **40**, 1040 (1989)
14. B. Krippa, M.C. Birse, J.A. McGovern, and N.R. Walet: Phys. Rev C **67**, 031301 (2003)
15. J. Carlson, V.R. Pandharipande, and R.B. Wiringa: Nucl. Phys. A **401**, 59 (1983)
16. S.L. Shapiro and S.A. Teukolsky: *Black Holes, White Dwarfs and Neutron Stars*, (John Wiley & Sons, New York, 1983)
17. P. Maessen, T. Rijken, and J. de Swart: Phys. Rev. C **40**, 2226 (1989)
18. M. Baldo, I. Bombaci, and G.F. Burgio: Astron. and Astr. **328**, 274 (1997)
19. M. Baldo, G.F. Burgio, and H.-J. Schulze: Phys. Rev. **61C**, 055801 (2000)
20. J.W. Negele and D. Vautherin: Nucl. Phys. A **207**, 298 (1973)
21. R. Feynman, F. Metropolis, and E. Teller: Phys. Rev. **75**, 1561 (1949)
22. G. Baym, C. Pethick, and D. Sutherland: Astrophys. J. **170**, 299 (1971)
23. A. Chodos, R.L. Jaffe, K. Johnson, C.B. Thorn, and V.F. Weisskopf: Phys. Rev. D **9**, 3471 (1974)
24. M. and S. Reddy: Phys. Rev. **67C**, 074024 (2003)
25. A. Akmal and V.R. Pandharipande: Phys. Rev. C **56**, 2261 (1997)
26. M. Alford, K. Rajagopal, and F. Wilczek: Phys. Lett. B **422**, 247 (1998)
27. M. Alford, K. Rajagopal, and F. Wilczek: Nucl. Phys. B **537**, 443 (1999)
28. M. Alford: Ann. Rev. Nucl. Part. Sci. **51**, 131 (2001)
29. G.F. Burgio, M. Baldo, P.K. Sahu, A.B. Santra, and H.-J. Schulze: Phys. Lett. B **562**, 19 (2002)
30. M. Baldo and G.F. Burgio: *Microscopic Theory of the Nuclear equation of State and Neutron Star Structure*, in "Physics of Neutron Star Interiors", Eds. D. Blaschke, N. Glendenning, and A. Sedrakian, Lectures Notes in Physics, Springer, vol. 578 (2001), pp. 1-30
31. R.A. Hulse and J.H. Taylor: Astrophys. J. **195**, L51 (1975)
32. N.K. Glendenning: Phys. Rev. D **46**, 1274 (1992)
33. P.K. Sahu: Phys. Rev. C **62**, 045801 (2000)
34. P.K. Sahu and A. Ohnishi: Nucl. Phys. A **691**, 439 (2001)
35. T. Hatsuda and T. Kunihiro: Phys. Rep. **247**, 221 (1994)
36. M. Buballa and M. Oertel: Nucl. Phys. A **703**, 770 (2002)
37. N.K. Glendenning: Compact Stars (Springer, New York, 1996)
38. Burgio, M. Baldo, P.K. Sahu and H.-J. Schulze: Phys. Rev. C **66**, 025802 (2002)